International Journal of Control and Automation
Vol.7, No.4 (2014), pp.113-124
http://dx.doi.org/10.14257/ijca.2014.7.4.11

A Practical Scheme for Induction Motor Modelling and Speed Control

Xinxin Shi[1,*], Hongsheng Li[1] and Jiacai Huang[1]

[1]*School of Automation, Nanjing Institute of Technology, No. 1 Hongjing Road, Nanjing 211167, P.R. China*

[*]*Corresponding author: sxx@njit.edu.cn*

Abstract

A practical scheme for induction motor modelling and speed control based on field oriented control is presented in this paper. Simplified model of the induction motor is constructed for simulations, which is time-saving and very suitable for controller design in Matlab/Simulink. Actual rotor speed signal is measured to modify the original rotor flux observer, which cannot perform well at low speeds, and conventional proportional-integral controllers are used in both speed and current loops for a desired speed. Comparative simulations and experimental results demonstrate the effectiveness of the proposed scheme, and the induction motor performs well at both high and low speeds.

Keywords: *induction motor; speed control; rotor flux observer; field oriented control; simulation model.*

1. Introduction

In modern industry, the majority of industrial applications use induction motors due to their high reliability, high efficiency and low prices [1]. Typical applications are robots, manufacturing automation, automobiles and so on [2, 3]. However, the control of induction motors is a challenging task because of their complex mathematical models, coupled torque and flux, and nonlinear behavior influenced by the working environment, such as external disturbances and parameter variations[4, 5].

Field oriented control (FOC), also called vector control, is the most widely used alternating current (AC) machine control method in high performance industrial applications [6]. FOC of an induction motor provides the decoupling between the torque and flux in the similar way as in a direct current (DC) machine. However, as the key component in FOC, the rotor flux is usually estimated by a flux observer, which requires accurate motor model [7]. Any parameter variation will lead to flux estimation error, and therefore the control performance decreases [8].

There are many types of flux estimate models, which usually are classified in terms of the input signals used, such as current model and voltage model observers [9, 10]. Since these flux models are very sensitive to motor parameters changes, advanced observer technique and adaptive control algorithm can be used [11]. An adaptive sliding rotor-flux observer was presented in [12], which was provided with an adaptive mechanism of rotor resistance. Simple and effective design criteria of rotor flux reduced-order observers for induction motors were proposed in [13], and a sensitivity analysis was carried out in the presence of variations of all the motor parameters.

ISSN: 2005-4297 IJCA

Numerous methods for induction machine online and offline parameter estimation were reviewed in [14], and parameter sensitivity analyses of full-order flux observers were given in [15]. Online estimation of states and parameters of an induction motor with Kalman filter was presented in [16], and a suitable methodology was proposed to ensure a good level of estimation accuracy. Parallel identification schemes for both speed and stator resistance were implemented in [17], and a sliding-mode current observer was combined with Popov's hyperstability theory in the estimation algorithm.

In most cases, the motor speed is the important variable, which usually needs to be maintained at a given constant, no matter whether the disturbance exists. Therefore, more and more advanced speed controllers based on modern control theory have been applied to induction motors, such as optimal control, adaptive control, variable structure control, neural network control and so on [18]. A synthesized method for speed control of induction motors based on optimal preview control system theory was implemented in [19]. A robust output feedback controller based on sliding modes and indirect adaptive control can be also applied to induction motor speed control, which has remarkable stability properties and offers a straightforward and intuitive tuning of its parameters [20].

In consideration of the possibility of existing speed sensor noise, maintenance and cost, the trend is to substitute computational solutions for speed sensors. Various speed sensorless controllers of induction motors have been researched, which can operate in a wide speed region [21].

A practical scheme for induction motor modelling and speed control is presented in this paper. Since the operating efficiency of the original asynchronous machine model in Matlab/Simulink software is not very high, a simple and efficient model of the induction motor has been constructed for simulation. Proportional–integral (PI) speed controller together with a modified rotor flux observer (MRFO) is implemented for both high and low speed operation. Comparative simulation and experimental results indicate the effectiveness of the proposed scheme.

2. Mathematical Model of the Induction Motor

The equivalent mathematical model of the induction motor in a two-phase stationary reference frame (α-β), under assumptions of linear magnetic circuits and balanced operating conditions, is presented as the following.

Phase voltage equations are

$$\begin{cases} u_{s\alpha} = R_s \cdot i_{s\alpha} + \mathrm{d}\varphi_{s\alpha}/\mathrm{d}t \\ u_{s\beta} = R_s \cdot i_{s\beta} + \mathrm{d}\varphi_{s\beta}/\mathrm{d}t \\ u_{r\alpha} = R_r \cdot i_{r\alpha} + \omega_r \cdot \varphi_{r\beta} + \mathrm{d}\varphi_{r\alpha}/\mathrm{d}t \\ u_{r\beta} = R_r \cdot i_{r\beta} - \omega_r \cdot \varphi_{r\alpha} + \mathrm{d}\varphi_{r\beta}/\mathrm{d}t \end{cases}, \quad (1)$$

where (R_s, R_r) represent the stator resistance and rotor resistance. ($u_{s\alpha}$, $u_{s\beta}$), ($i_{s\alpha}$, $i_{s\beta}$) and ($\varphi_{s\alpha}$, $\varphi_{s\beta}$) are the stator voltages, currents and fluxes respectively. ($u_{r\alpha}$, $u_{r\beta}$), ($i_{r\alpha}$, $i_{r\beta}$) and ($\varphi_{r\alpha}$, $\varphi_{r\beta}$) are the rotor voltages, currents and fluxes respectively. ω_r is the electrical rotor speed.

The flux equations are

$$\begin{cases} \varphi_{s\alpha} = L_s \cdot i_{s\alpha} + L_m \cdot i_{r\alpha} \\ \varphi_{s\beta} = L_s \cdot i_{s\beta} + L_m \cdot i_{r\beta} \\ \varphi_{r\alpha} = L_r \cdot i_{r\alpha} + L_m \cdot i_{s\alpha} \\ \varphi_{r\beta} = L_r \cdot i_{r\beta} + L_m \cdot i_{s\beta} \end{cases}, \tag{2}$$

where L_m is the mutual inductance, L_s and L_r are the total stator and rotor inductances, which are the sums of the mutual inductance and leakage inductances (L_{ls}, L_{lr}) respectively.

Torque and motion equations are

$$\begin{cases} T_e = p \cdot (\varphi_{s\alpha} \cdot i_{s\beta} - \varphi_{s\beta} \cdot i_{s\alpha}) \\ \dfrac{d\omega}{dt} = \dfrac{1}{J}(T_e - T_m - F \cdot \omega) \\ \omega_r = p \cdot \omega \end{cases}, \tag{3}$$

where T_e is the electromagnetic torque, p is the number of pole pairs, ω is the mechanical rotor speed, T_m is the shaft mechanical torque, J is the load inertia and F is the viscous friction coefficient.

It can be seen from equations (1)-(3) that the induction motor is a highly coupled, nonlinear and complex system.

3. Scheme for Induction Motor Modelling and Speed Control

3.1. Modelling details

According to equations (1)-(3), simulation model of induction motors in Matlab/Simulink can be constructed as follows. Total topology of the model is shown in Figure 1.

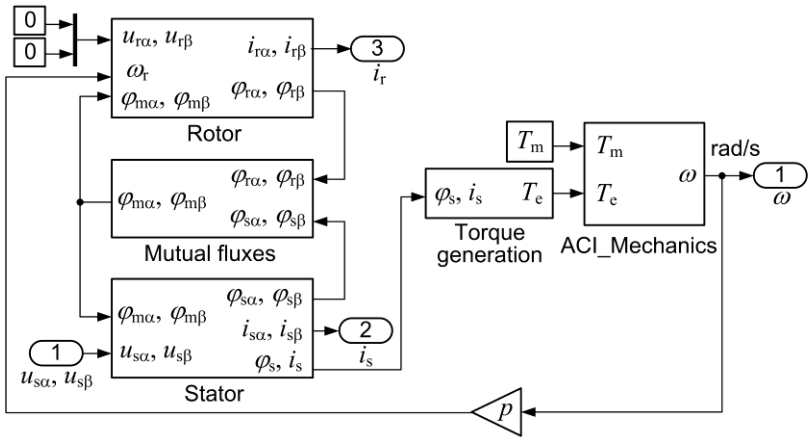

Figure 1. Total topology of the induction motor model

On the basis of following equations

$$\begin{cases} L_s = L_{ls} + L_m \\ L_r = L_{lr} + L_m \\ \varphi_{m\alpha} = L_m \cdot (i_{s\alpha} + i_{r\alpha}) \\ \varphi_{m\beta} = L_m \cdot (i_{s\beta} + i_{r\beta}) \end{cases}, \tag{4}$$

equation (2) can be rewritten as

$$\begin{cases} \varphi_{s\alpha} = L_{ls} \cdot i_{s\alpha} + \varphi_{m\alpha} \\ \varphi_{s\beta} = L_{ls} \cdot i_{s\beta} + \varphi_{m\beta} \\ \varphi_{r\alpha} = L_{lr} \cdot i_{r\alpha} + \varphi_{m\alpha} \\ \varphi_{r\beta} = L_{lr} \cdot i_{r\beta} + \varphi_{m\beta} \\ \varphi_{m\alpha} \cdot \left(\frac{1}{L_{ls}} + \frac{1}{L_m} + \frac{1}{L_{lr}} \right) = \left(\frac{\varphi_{s\alpha}}{L_{ls}} + \frac{\varphi_{r\alpha}}{L_{lr}} \right) \\ \varphi_{m\beta} \cdot \left(\frac{1}{L_{ls}} + \frac{1}{L_m} + \frac{1}{L_{lr}} \right) = \left(\frac{\varphi_{s\beta}}{L_{ls}} + \frac{\varphi_{r\beta}}{L_{lr}} \right) \end{cases}. \tag{5}$$

Therefore, the stator and rotor dynamics are modelled in Figure 2.

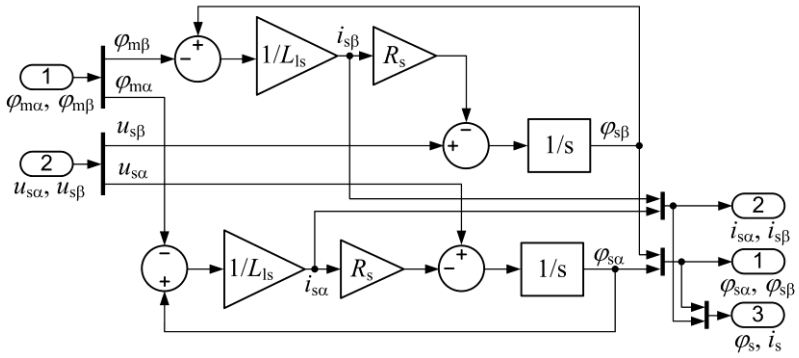

(a)

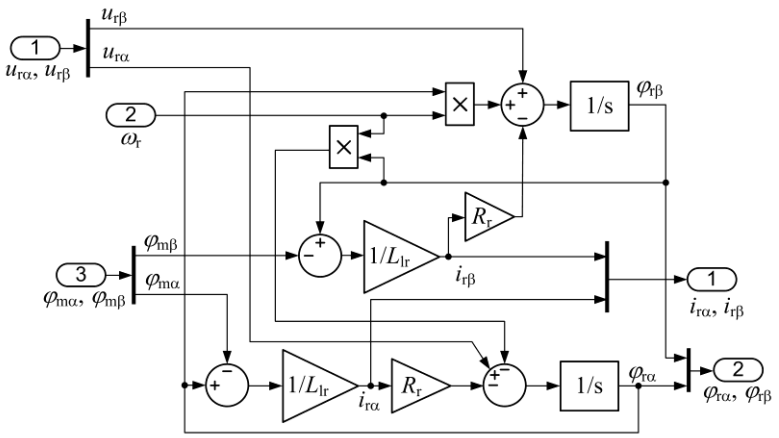

(b)

Figure 2. Dynamic model of induction motors (a) Stator (b) Rotor

Other modules in the induction motor model, such as the torque generation, mechanics, and mutual fluxes modules, are very simple to construct based on equations (3) and (5).

3.2. Speed control system design

The practical speed control system of the induction motor is illustrated in Figure 3, which consists of rotor flux observer, current and speed loops.

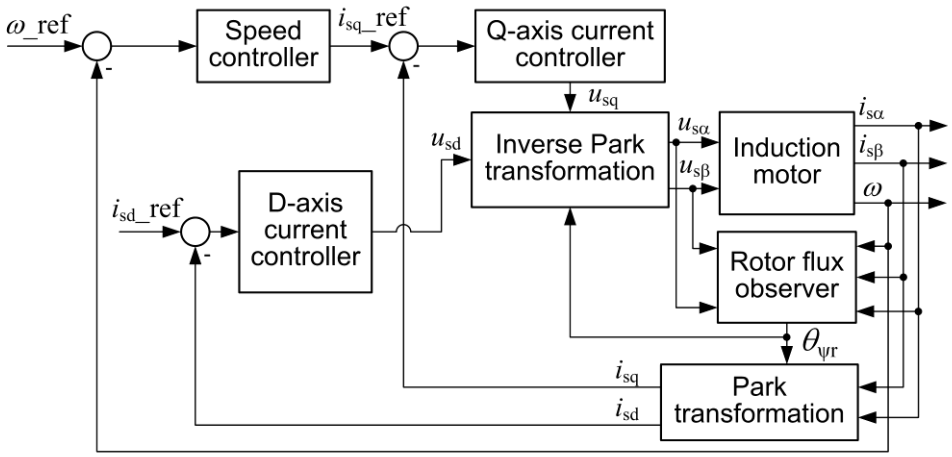

Figure 3. Practical speed control system of the induction motor

The rotor flux observer is modified based on [22], the goal of which is to provide actual rotor flux angle for Park transformation. The MRFO in stationary reference frame can be discretized as follows.

$$\begin{aligned}\psi_{r\alpha}^{i}(k) &= \psi_{r\alpha}^{i}(k-1) + T\cdot\left(\frac{L_m\cdot R_r}{L_r}\cdot i_{s\alpha}(k) - \frac{R_r}{L_r}\cdot\psi_{r\alpha}^{i}(k-1) - \omega_r(k)\cdot\psi_{r\beta}^{i}(k-1)\right)\\ \psi_{r\beta}^{i}(k) &= \psi_{r\beta}^{i}(k-1) + T\cdot\left(\frac{L_m\cdot R_r}{L_r}\cdot i_{s\beta}(k) - \frac{R_r}{L_r}\cdot\psi_{r\beta}^{i}(k-1) + \omega_r(k)\cdot\psi_{r\alpha}^{i}(k-1)\right)\end{aligned}, \quad (6)$$

where k represents the kth sampling instant; (k - 1) represents the (k - 1)th sampling instant; T is the sampling period; ($\psi_{r\alpha}^{i}$, $\psi_{r\beta}^{i}$) are stationary α-axis and β-axis rotor fluxes in current model.

Since the current model cannot work very well at higher speed, the voltage model of the rotor flux is presented to guarantee better accuracy:

$$\begin{aligned}\psi_{r\alpha}^{v}(k) &= -\left(\frac{L_s\cdot L_r - L_m\cdot L_m}{L_m}\right)\cdot i_{s\alpha}(k) + \frac{L_r}{L_m}\cdot\psi_{s\alpha}^{v}(k)\\ \psi_{r\beta}^{v}(k) &= -\left(\frac{L_s\cdot L_r - L_m\cdot L_m}{L_m}\right)\cdot i_{s\beta}(k) + \frac{L_r}{L_m}\cdot\psi_{s\beta}^{v}(k)\end{aligned}, \quad (7)$$

where ($\psi_{r\alpha}^{v}$, $\psi_{r\beta}^{v}$) are stationary α-axis and β-axis rotor fluxes in voltage model, ($\psi_{s\alpha}^{v}$, $\psi_{s\beta}^{v}$) are stationary α-axis and β-axis stator fluxes, which are discretized by using trapezoidal approximation as

$$\begin{aligned}
\psi_{s\alpha}^{v}(k) &= \psi_{s\alpha}^{v}(k-1) + \frac{T}{2}\cdot\left[e_{s\alpha}(k) + e_{s\alpha}(k-1)\right] \\
\psi_{s\beta}^{v}(k) &= \psi_{s\beta}^{v}(k-1) + \frac{T}{2}\cdot\left[e_{s\beta}(k) + e_{s\beta}(k-1)\right], \\
e_{s\alpha}(k) &= u_{s\alpha}(k) - R_s\cdot i_{s\alpha}(k) + u_{comp,\,r\alpha}(k) \\
e_{s\beta}(k) &= u_{s\beta}(k) - R_s\cdot i_{s\beta}(k) + u_{comp,\,r\beta}(k)
\end{aligned} \tag{8}$$

where ($e_{s\alpha}$, $e_{s\beta}$) are the back electromotive forces, ($u_{comp,\,r\alpha}$, $u_{comp,\,r\beta}$) are the compensation voltages designed by the PI controller, which are given as follows:

$$\begin{aligned}
u_{comp,\,r\alpha}(k) &= K_P\cdot\left[\psi_{r\alpha}^{i}(k) - \psi_{r\alpha}^{v}(k)\right] + u_{comp,\,r\alpha,\,i}(k-1) \\
u_{comp,\,r\beta}(k) &= K_P\cdot\left[\psi_{r\beta}^{i}(k) - \psi_{r\beta}^{v}(k)\right] + u_{comp,\,r\beta,\,i}(k-1) \\
u_{comp,\,r\alpha,\,i}(k) &= u_{comp,\,r\alpha,\,i}(k-1) + K_I\cdot T\cdot\left[\psi_{r\alpha}^{i}(k) - \psi_{r\alpha}^{v}(k)\right], \\
u_{comp,\,r\beta,\,i}(k) &= u_{comp,\,r\beta,\,i}(k-1) + K_I\cdot T\cdot\left[\psi_{r\beta}^{i}(k) - \psi_{r\beta}^{v}(k)\right]
\end{aligned} \tag{9}$$

where $u_{comp,\,r\alpha,\,i}(k-1)$ and $u_{comp,\,r\beta,\,i}(k-1)$ are integral components, K_P and K_I are the proportional and integral gains respectively.

Therefore, the rotor flux angle $\theta_{\psi r}$ is finally computed as

$$\theta_{\psi r}(k) = \tan^{-1}\left(\frac{\psi_{r\beta}^{v}(k)}{\psi_{r\alpha}^{v}(k)}\right). \tag{10}$$

Well-tuned PI controllers are used in speed and current loops respectively. Here, classical PI controller is adopted which can be designed as follows.

$$\begin{cases} e(k) = y_d(k) - y(k) \\ u(k) = K_p\cdot e(k) + K_i\cdot\sum_{j=1}^{k} e(j)\cdot T \end{cases}, \tag{11}$$

where y_d is the desired speed or current, y is the actual speed or current, e is the error between desired and actual values, K_p and K_i are controller parameters, and u is the control input.

4. Comparative Simulations

4.1. Modelling comparisons

To indicate the correctness of the constructed induction motor model, comparative simulations with the original asynchronous machine block in Matlab/Simulink are illustrated in Figure 4. The given stator voltages are $u_{s\alpha} = 375\sin(120\pi t + 0.5\pi)$ (V) and $u_{s\beta} = 375\sin(120\pi t)$ (V). Parameter values of the induction motor are given in Table 1.

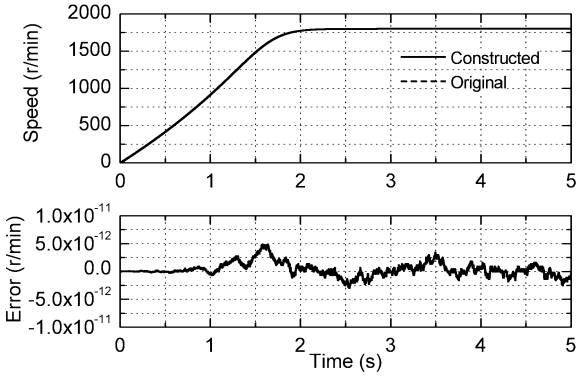

Figure 4. Comparative simulations between the constructed induction motor model and the original block

Table 1. Parameter values of the induction motor

Items	Values
Stator resistance (R_s)	11.05 Ω
Rotor resistance (R_r)	6.11 Ω
Mutual inductance (L_m)	0.293939 H
Stator inductance (L_s)	0.316423 H
Rotor inductance (L_r)	0.316423 H
Number of pole pairs (p)	2
Load inertia (J)	0.0006 $kg \cdot m^2$
Viscous friction coefficient (F)	0.0008 $(N \cdot m)/(rad/s)$

It can be seen from Figure 4 that two rotor speeds coincide with each other very well, which indicates that these two models are the same. Moreover, running the constructed induction motor model in Matlab/Simulink is time-saving when compared with the original one, which is very suitable for controller design.

4.2. Control system comparisons

The performance of the proposed scheme for controlling induction motors will be tested in comparison with another rotor flux observer, in which the rotor speed signal is not used. The following two control systems are compared in detail.

(1) PI + MRFO: the same as that described in Section 3.2.

(2) PI + RFO: differences between these two observers are the signal used and the compensation voltage calculation method. In MRFO, the measured speed signal and rotor flux modelling error are used, while in RFO, the stator flux modelling error is used without speed signal. The stationary α-axis and β-axis stator fluxes in the voltage model ($\psi_{s\alpha}^{v}$, $\psi_{s\beta}^{v}$) are expressed in equation (8). In the current model, the stator flux is given as

$$\begin{aligned}\psi_{s\alpha}^{i}(k)&=\left(\frac{L_s\cdot L_r-L_m\cdot L_m}{L_r}\right)\cdot i_{s\alpha}(k)+\frac{L_m}{L_r}\cdot\psi_{r\alpha}^{i}(k)\\ \psi_{s\beta}^{i}(k)&=\left(\frac{L_s\cdot L_r-L_m\cdot L_m}{L_r}\right)\cdot i_{s\beta}(k)+\frac{L_m}{L_r}\cdot\psi_{r\beta}^{i}(k)\end{aligned}. \tag{12}$$

($\psi_{r\alpha}^{i}$, $\psi_{r\beta}^{i}$) are established from

$$\begin{aligned}\psi_{r\alpha}^{i}(k)&=\psi_{r}^{e}(k)\cdot\cos(\theta_{\psi r}(k))\\ \psi_{r\beta}^{i}(k)&=\psi_{r}^{e}(k)\cdot\sin(\theta_{\psi r}(k))\end{aligned}, \tag{13}$$

where $\psi_{r}^{e}(k)$ is the total rotor flux linkage which is aligned into the *d*-axis in synchronously rotating reference frame. The oriented rotor flux dynamics are

$$\psi_{r}^{e}(k)=\left(\frac{L_r}{L_r+R_r\cdot T}\right)\cdot\psi_{r}^{e}(k-1)+\left(\frac{L_m\cdot R_r\cdot T}{L_r+R_r\cdot T}\right)\cdot i_{sd}^{e}(k), \tag{14}$$

where i_{sd}^{e} is the *d*-axis stator current in synchronously rotating reference frame.

According to the tuning methods presented in [23], final controller parameter values are determined by trial and error. PI gains in the speed loop are K_p = 2, K_i = 0.002, T = 0.0001, and PI gains in the current loop are K_p = 1, K_i = 0.025, T = 0.0001. In addition, PI gains in the rotor flux observer are K_P = 2.8, K_I = 6.2, and the sampling period T is 0.0001 s.

Desired speeds are given as 1080 r/min, 1800 r/min, 72 r/min, and 3.6 r/min respectively to test the controller performance at both high and low speeds. Comparative simulation results between the two aforementioned controllers are illustrated in Figure 5.

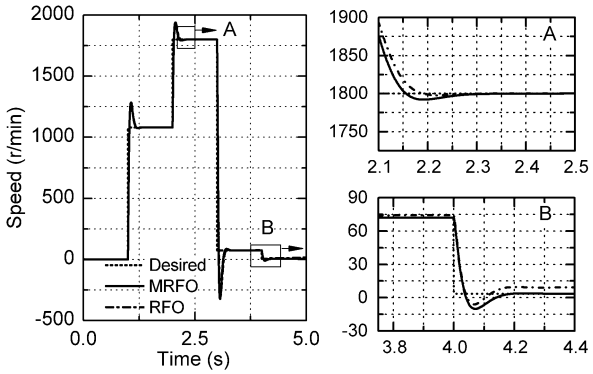

Figure 5. Comparative simulation results at different speeds

It can be seen from Figure 5 that both controllers perform well at high speeds. There is a relative big tracking error at low speeds in the RFO based control system, while MRFO based control system can achieve good performance at both high and low speeds.

5. Experimental Results

5.1. Experimental setup

To test the performance of the proposed scheme in practice, experiments were carried out on an induction motor with the same parameters given in Table 1. Experimental setup of the induction motor control system is shown in Figure 6, which is based on a high voltage motor control developers kit produced by Texas Instruments Company. Sampling periods of current and position loops are both 0.0001 s. Experimental data are captured for display and analysis via a graph tool in the code composer studio (CCS).

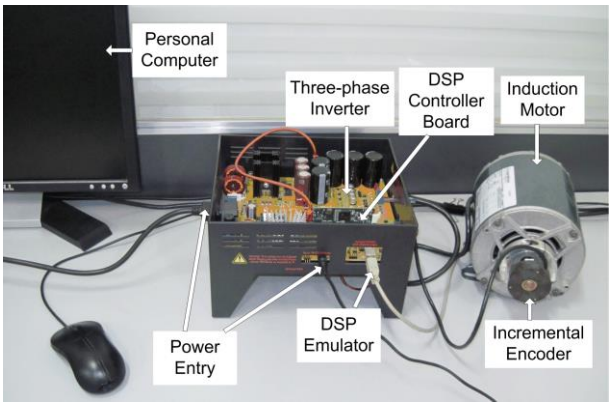

(a)

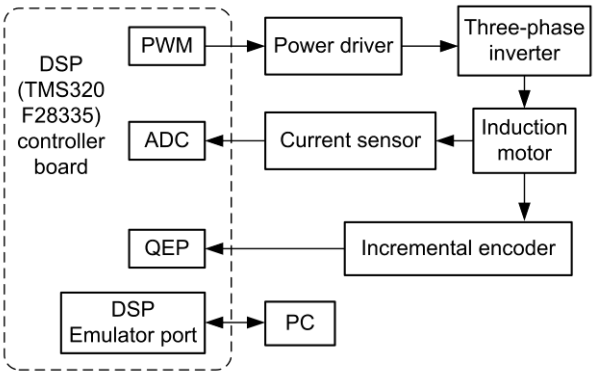

(b)

Figure 6. Experimental setup of the induction motor control system (a) Actual (b) Schematic

5.2. Results and discussion

Experimental results are given in Figure 7.

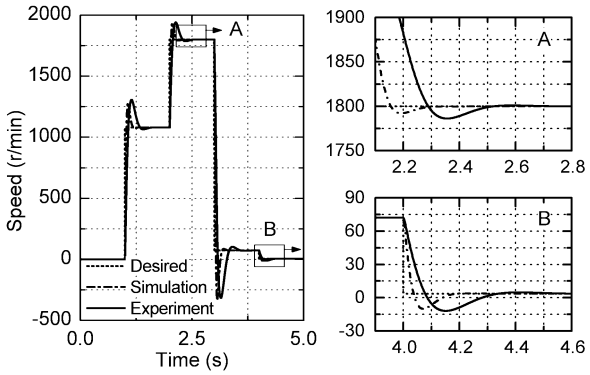

Figure 7. Experimental results at different speeds

It can be seen from Figure 7 that the induction motor tracks the desired speeds well in a wide range, which demonstrates the effectiveness of the proposed scheme. Step response in experimental results is not as fast as that in simulations due to the actual complex system and unmodelled dynamics. Moreover, a small overshoot exists at the beginning of the step response curve owing to the simple motion controller.

6. Conclusions

Simplified models and speed control of induction motors based on modified rotor flux observer are explored in this paper. Simulations based on simplified models of induction motors are very time-saving, which benefit the controller design especially. Furthermore, actual rotor speed signal is used in the rotor flux observer to obtain excellent performance at both high and low speeds. The limitation of this method is that the rotor speed must be measured for rotor flux observer and speed control, so it is not suitable for sensorless system. Comparative simulations and experimental results indicate the effectiveness of the proposed scheme, and the induction motor can realize the desired motion well. Consequently, the simplified model and modified rotor flux observer provide a new practical solution for high-performance speed control of induction motors. In future work, advanced motion control algorithms can be combined with the MRFO to achieve better performance.

Acknowledgements

This work was supported by the Natural Science Foundation of Jiangsu Province, China [grant number BK20130744]; the Scientific Research Foundation of Nanjing Institute of Technology [grant number YKJ201220]; the National Natural Science Foundation of China [grant number 61104085]; and the Scientific Research Foundation of Jiangsu Province, China [grant number 11KJB510005]. The authors would like to express their appreciation to the sponsors.

References

[1] B. Gasbaoui, A. Nasri, A. Laoufi and Y. Mouloudi, "4 WD urban electric vehicle motion studies based on MIMO fuzzy logic speed controller", International Journal of Control and Automation, vol. 6, no. 1, **(2013)**, pp. 105-118.
[2] O. S. Ebrahim, M. A. Badr, A. S. Elgendy and P. K. Jain, "ANN-based optimal energy control of induction motor drive in pumping applications", IEEE Transactions on Energy Conversion, vol. 25, no. 3, **(2010)**, pp. 652-660.

[3] Q. Lu, Y. Li, Y. Ye and Z. Q. Zhu, "Investigation of forces in linear induction motor under different slip frequency for low-speed maglev application", IEEE Transactions on Energy Conversion, vol. 28, no. 1, **(2013)**, pp. 145-153.
[4] H. Kraiem, A. Flah, M. B. Hamed and L. Sbita, "High performances induction motor drive based on fuzzy logic control", International Journal of Control and Automation, vol. 5, no. 1, **(2012)**, pp. 1-12.
[5] A. N. Lakhal, A. S. Tlili and B. N. Braiek, "Neural network observer for nonlinear systems application to inductio motors", International Journal of Control and Automation, vol. 3, no. 1, **(2010)**, pp. 1-16.
[6] V. F. Victor, F. O. Quintaes, J. S. B. Lopes, L. D. S. Junior, A. S. Lock and A. O. Salazar, "Analysis and study of a bearingless AC motor type divided winding, based on a conventional squirrel cage induction motor", IEEE Transactions on Magnetics, vol. 48, no. 11, **(2012)**, pp. 3571-3574.
[7] C. Korlinchak and M. Comanescu, "Robust sensorless sliding mode flux observer with speed estimate for induction motor drives", Electric Power Components and Systems, vol. 40, no. 9, **(2012)**, pp. 1030-1049.
[8] S. H. Jeon, K. K. Oh and J. Y. Choi, "Flux observer with online tuning of stator and rotor resistances for induction motors", IEEE Transactions on Industrial Electronics, vol. 49, no. 3, **(2002)**, pp. 653-664.
[9] M. P. Kazmierkowski, L. G. Franquelo, J. Rodriguez, M. A. Perez and J. I. Leon, "High-performance motor drives", IEEE Industrial Electronics Magazine, vol. 5, no. 3, **(2011)**, pp. 6-26.
[10] P. L. Jansen and R. D. Lorenz, "A physically insightful approach to the design and accuracy assessment of flux observers for field oriented induction machine drives", IEEE Transactions on Industry Applications, vol. 30, no. 1, **(1994)**, pp. 101-110.
[11] S. Bolognani, L. Peretti and M. Zigliotto, "Parameter sensitivity analysis of an improved open-loop speed estimate for induction motor drives", IEEE Transactions on Power Electronics, vol. 23, no. 4, **(2008)**, pp. 2127-2135.
[12] R. Trabelsi, A. Khedher, M. F. Mimouni and F. M'sahli, "Backstepping control for an induction motor using an adaptive sliding rotor-flux observer", Electric Power Systems Research, vol. 93, no. **(2012)**, pp. 1-15.
[13] F. Alonge and F. D'Ippolito, "Design and sensitivity analysis of a reduced-order rotor flux optimal observer for induction motor control", Control Engineering Practice, vol. 15, no. **(2007)**, pp. 1508-1519.
[14] H. A. Toliyat, E. Levi and M. Raina, "A review of RFO induction motor parameter estimation techniques", IEEE Transactions on Energy Conversion, vol. 18, no. 2, **(2003)**, pp. 271-283.
[15] M. Hinkkanen and J. Luomi, "Parameter sensitivity of full-order flux observers for induction motors", IEEE Transactions on Industry Applications, vol. 39, no. 4, **(2003)**, pp. 1127-1135.
[16] E. Laroche, E. Sedda and C. Durieu, "Methodological insights for online estimation of induction motor parameters", IEEE Transactions on Control Systems Technology, vol. 16, no. 5, **(2008)**, pp. 1021-1028.
[17] M. S. Zaky, M. M. Khater, S. S. Shokralla and H. A. Yasin, "Wide-speed-range estimation with online parameter identification schemes of sensorless induction motor drives", IEEE Transactions on Industrial Electronics, vol. 56, no. 5, **(2009)**, pp. 1609-1707.
[18] J. A. Riveros, F. Barrero, E. Levi, M. J. Duran, S. Toral and M. Jones, "Variable-speed five-phase induction motor drive based on predictive torque control", IEEE Transactions on Industrial Electronics, vol. 60, no. 8, **(2013)**, pp. 2957-2968.
[19] M. M. M. Negm, J. M. Bakhashwain and M. H. Shwehdi, "Speed control of a three-phase induction motor based on robust optimal preview control theory", IEEE Transactions on Energy Conversion, vol. 21, no. 1, **(2006)**, pp. 77-84.
[20] J. B. Oliveira, A. D. Araujo and S. M. Dias, "Controlling the speed of a three-phase induction motor using a simplified indirect adaptive sliding mode scheme", Control Engineering Practice, vol. 18, no. 6, **(2010)**, pp. 577-584.
[21] J. Guzinski and H. Abu-Rub, "Speed sensorless induction motor drive with predictive current controller", IEEE Transactions on Industrial Electronics, vol. 60, no. 2, **(2013)**, pp. 699-709.
[22] P. L. Jansen, C. O. Thompson and R. D. Lorenz, "High-quality torque control at zero and very high speed operation", IEEE Industry Applications Magazine, vol. no. **(1995)**, pp. 7-13.
[23] P. Cominos and N. Munro, "PID controllers: recent tuning methods and design to specification", IEE Proceedings Control Theory and Applications, vol. 149, no. 1, **(2002)**, pp. 46-53.

Authors

Xinxin Shi

Xinxin Shi received the B.Eng. and Ph.D. degrees in mechatronic control engineering from Nanjing University of Science and Technology, Nanjing, China, in 2007 and 2012, respectively. She is currently a Lecturer in the School of Automation, Nanjing Institute of Technology, Nanjing, China. Her research interests include motion control of induction motors, precision motion control of electromagnetic linear actuator, active disturbance rejection control, and robotics.

Hongsheng Li

Hongsheng Li received the Ph.D. degree in control science and engineering from SouthEast University, Nanjing, China, in 2005. He is currently a Professor in the School of Automation, Nanjing Institute of Technology, Nanjing, China. He has finished two important national projects and numerous local projects. His research interests include motion control of induction motors, fractional order control, iterative learning control, and robotics.

Jiacai Huang

Jiacai Huang received the B.Eng., M.Eng., and Ph.D. degrees in control theory and engineering from Jilin University, Changchun, China, in 2000, 2003, and 2006, respectively. He is currently a Professor in the School of Automation, Nanjing Institute of Technology, Nanjin7g, China. His research interests include motion control of induction motors, intelligent control, and signal processing.